Journal of King Saud University – Science 32 (2020) 2406–2413

Contents lists available at ScienceDirect

Journal of King Saud University – Science

journal homepage: www.sciencedirect.com

Original article

In vitro mechanistic investigation of polycyclic cage-like heterocyclic hybrid possessing diverse pharmacophoric units

Raju Suresh Kumar *, Abdulrahman I. Almansour, Natarajan Arumugam

Department of Chemistry, College of Science, King Saud University, P.O. Box 2455, Riyadh 11451, Saudi Arabia

ARTICLE INFO

Article history:
Received 17 February 2020
Revised 8 March 2020
Accepted 17 March 2020
Available online 24 March 2020

Keywords:
Anticancer activity
Broad spectrum activity
[3 + 2] Cycloaddition
Annulation
Polycyclic cage-like heterocyclic hybrid

ABSTRACT

A novel polycyclic cage-like heterocyclic hybrid comprising several privileged structures such as pyrroloisoquinoline, 4-pyridinone and a α,β -unsaturated ketone moiety has been synthesized in good yield employing a microwave mediated [3 + 2]-cycloaddition/annulation strategy in 1-butyl-3-methylimidazolium bromide ([bmim]Br). The compound thus synthesized was analyzed for *in vitro* anticancer activity employing MCF-7, Jurkat, HCT 116 and NCI-H460 cell lines. The effect of polycyclic cage-like heterocyclic hybrid on cells viability was analyzed by MTT assay and its DNA damage efficiency was confirmed by several examinations like apoptosis study, cell cycle analysis, caspase-3 expression analysis and TUNEL assay. Mitochondrial membrane potential was determined by JC-1 staining. The polycyclic cage-like heterocyclic hybrid bearing diverse functionalities played a major role in DNA damage of cancerous cells and in consequence inhibited the DNA cells proliferation.

1. Introduction

Cancer is a somber bug which affects more or less every tissue line in human body and imposes immense challenges to health sciences (Varmus, 2006). It has become a reason for principal causes of casualties in developed and underdeveloped countries (Saleem et al., 2013). 5-Fluorouracil, cisplatin, taxol etc are some of the naturally available and synthetic anticancer drugs (Ali et al., 2017). Severe side effects like solubility and biocompatibility issues, cytotoxicities induction and constricted therapeutic frame are observed with most of the available anticancer drugs (Pulkkinen et al., 2008) and hence a demand for the invention of novel anticancer drug which could restrict the proliferative pathways has been increasing constantly. Anticancer drugs are usually used as stimulant medicine against diverse cancers in sequence with surgery as well as radiation therapy (Fukusumi et al., 2019). Drugs used in chemotherapy follow several ways to treat cancer. They usually affect rapid division of cells or target the food supply of cancer cells, hamper the DNA replications process, interact with several proteins causing cell division (Ali et al., 2016). Chemoresistance has been a major reason for failure of chemotherapy (Hamilton and Rath, 2014). Conversely, the need for anticancer drugs which could treat the later stages of cancer without any side effects is imperative. Nanoparticles derived from natural sources were used as anticancer agents (Alsalhi et al., 2016; Alfuraydi et al., 2019).

Molecules possessing multiple pharmacophoric units, in which each distinct active unit utilizes diverse means of action, could be of assistance in the treatment of intricate, multifactorial diseases such as cancer (Petrelli and Valabrega, 2009). In this regard, cage-like compounds with a closed cavity provide an opportunity to join several active units in a single compact structure (Geldenhuys et al., 2005) and can take part in molecular recognition process. Besides, the cage-like polycyclic heterocyclic compounds act as artificial receptors (Geldenhuys et al., 2005) and it is pertinent to note that an effective antitumor drug, Gambogic acid is a natural cage-like heterocyclic hybrid (Han and Xu, 2009; Boros et al., 2013; Yihebali et al, 2013). One of pharmacophoric unit viz. the quinoline derivatives are widely used as anticancer drugs and its analogues can inhibit the tubulin polymerization, tyrosine kinases, DNA repair and proteasome (Solomon and Lee, 2011; Solomon and Lee, 2009; Wissner and Mansour, 2008; Boschelli et al., 2002; Nien et al., 2010). Furthermore, analogues of pyridinone are also found to show great efficacy in anticancer activity (Lv et al., 2013; Androutsopoulos and Spandidos, 2018;

* Corresponding author.
E-mail address: sraju@ksu.edu.sa (R. Suresh Kumar).

Peer review under responsibility of King Saud University.

Production and hosting by Elsevier

https://doi.org/10.1016/j.jksus.2020.03.029
1018-3647/

Li et al., 2018). Protein expression changes, DNA damage and cell apoptosis are of major pathways of pyridinone derivatives for cancer cell proliferation inhibition (Rostom et al., 2011; Priyadarshani et al., 2016). Hence, we presume that the combination of these derivatives in a cage-like framework could treat cancer effectively.

On the other hand, reports on the anticancer studies of cage-like heterocycles comprising several pharmacophoric units in a single molecule are scarce in the literature. Hence in the present study, we planned to study the pharmacological profile and the mechanistic aspects of apoptosis of the synthesized compound as it possesses diverse structural units in a polycyclic cage-like framework and report the results in this article.

2. Experimental

2.1. Materials and methods

2.1.1. Chemistry

Melting point was recorded using open capillary tube and is uncorrected. ^{1}H, ^{13}C and two-dimensional NMR spectra were documented on a Bruker 500 MHz instrument in $CDCl_3$ using Tetramethylsilane (TMS) as internal standard and the standard Bruker software was employed. Chemical shifts are given in parts per million (δ-scale) and the coupling constants are given in Hertz. IR spectra were recorded on a Perkin Elmer system 2000 FT-IR instrument (KBr). Elemental analyses were done on a Perkin Elmer 2400 Series II Elemental CHNS analyzer.

*2.1.1.1. Experimental procedure for the synthesis of polycyclic cage-like heterocyclic hybrid **4**.* A 1:1:1 mixture of 3,5-bis[(*E*)-phenylmethylidene]tetrahydro-4(*1H*)-pyridinone **1**, acenaphthenequinone **2** and 1,2,3,4-tetrahydroisoquinoline-3-carboxylic acid **3** in 1-butyl-3-methylimidazolium bromide ([bmim]Br) (200 mg) was irradiated at 100 °C for 12 min in a CEM microwave synthesizer. After the reaction has been completed (TLC), 10 ml of ethyl acetate was added to the reaction mixture and stirred for 15 min. The ethyl acetate layer was then separated and washed with 50 ml of water and the solvent was evaporated under reduced pressure. The precipitate obtained was dried in vacuum and subjected to column chromatography for purification using petroleum ether–ethyl acetate mixture (6:4) to obtain the polycyclic cage-like heterocyclic hybrid **4** in pure form.

Obtained as pale brown solid, (Yield, 88%); mp = 174–176 °C; IR (KBr): 1598, 1685, 3427 cm^{-1}; ^{1}H NMR (500 MHz, $CDCl_3$): δ 2.86 (dd, 1H, *J* = 15.0, 14.0 Hz, H-18), 3.02 (d, 1H, *J* = 12.0 Hz, H-25), 3.07 (dd, 1H, *J* = 15.0, 5.0 Hz, H-18), 3.19 (d, 1H, *J* = 13.5 Hz, H-13), 3.39 (d, 1H, *J* = 17.5 Hz, H-24), 3.60–3.70 (m, 2H, H-13 and H-24), 4.27–4.29 (m, 2H, H-20 and H-25), 4.42–4.47 (m, 1H, H-19), 6.26 (s, 1H, H-26), 6.40 (d, 2H, *J* = 7.5 Hz, ArH), 6.72 (d, 1H, *J* = 7.0 Hz, ArH), 7.07–7.12 (m, 4H, ArH), 7.16 (d, 1H, *J* = 7.5 Hz, ArH), 7.21 (d, 1H, *J* = 7.5 Hz, ArH), 7.27–7.42 (m, 5H, ArH), 7.47–7.54 (m, 4H, ArH), 7.57 (d, 1H, *J* = 8.0 Hz, ArH), 7.71 (d, 1H, *J* = 8.0 Hz, ArH). ^{13}C NMR (125 MHz, $CDCl_3$): δ 34.48, 48.01, 52.46, 52.71, 56.45, 63.19, 72.76, 94.50, 121.12, 124.32, 125.80, 125.89, 126.34, 126.44, 127.45, 127.75, 128.54, 128.60, 128.99, 129.07, 129.55, 130.36, 130.47, 130.79, 133.03, 133.42, 133.85, 134.84, 135.14, 135.31, 135.74, 136.05, 136.74, 136.89, 138.48, 196.70. Anal. calcd for $C_{40}H_{32}N_2O_2$: C, 83.89; H, 5.63; N, 4.89%; found: C, 83.71; H, 5.84; N, 4.75%.

2.1.2. Biology

2.1.2.1. Cell culture. MNI-H460, human non-small cancer line was obtained from NCCS, Pune. The cell lines were cultured in DMEM media, which was supplemented with 10% Fetal Bovine Serum (FBS) and a combination of antibiotics, 100 U/mL streptomycin and 100 U/mL penicillin. Cells were suspended in cell culture flasks and incubated at 37 °C in 5% CO_2 humidified atmosphere. Cells were extracted when 80% confluency is reached. A cell counting was done with an aid of a Hemocytometer and assays were performed after calculating the viability and seeding the cells.

2.1.2.2. Cytotoxicity assay. Synthesized cage like compound was subjected to cytotoxicity test evaluated by MTT assay. A NCI-H460 cells suspension of 2×10^4 cells/well/200 μL of DMEM medium was added to 96-well plates and the growth is allowed for 12 h. Later, different concentrations of test compound varied from 1 to20 μM, with a step size of 5 μM were added to every well. After incubating for 78 h in 5% CO_2 atmosphere, spent medium was removed. MTT reagent of 20 μL, 5 mg/mL was added to the cells and further incubated in CO_2 incubator for 2 h. The formazan crystals were dissolved in DMSO, 100 μL and the absorbance was measured to 570 nm using microplate reader. The CPT alone treated cells were regarded as positive control with 100% viability. % of cell viability was calculated using Eq. (1).

$$\%\,viability = \left(\frac{Mean\ absorbance\ of\ test\ sample}{Mean\ absorbance\ of\ negati\,ve\ control}\right) \times 100 \qquad (1)$$

2.1.2.3. Apoptosis assay. MCF-7 cells of density 1×10^6 cells/well were plated for 12 h and then cultured for 48 h in a medium of known drug concentrations. Annexin V/FITC Kit from BD Biosciences, Catalog no. 556547 was used to perform apoptosis assay. FITC-conjugated annexin V and PI fluorescence intensities in cells were examined by flow cytometry. Cultured test materials were then collected and washed with PBS buffer and were resuspended in annexin V-FITC buffer. The suspension was incubated at 25 °C for 10 min in dark with annexin V-FITC of 5 μL. The cells were collected by centrifugation, resuspended in annexin V-FITC buffer and PI of 5 μL was added in ice bath. Flow cytometry Cell Quest software (Becton Dickinson Biosciences) was used for further analysis. All experiments were repeated and the data was presented with ± STD.

2.1.2.4. Cell cycle analysis. MCF-7 cells (1×10^6 cells/well) were traced with test drugs and incubated for 48 h. Cells were removed, washed with PBS and fixed in ethanol of 70%, for 30 min at −20 °C. After that both treated and untreated cells were again washed with PBS and RNase A (50 μL) was directly added to pellet. Cells were co-incubated in room temperature with PI solution (400 μL/million cells) for 5–10 min. BD FACS Callibur flow cytometry with Cell Quest software was used to determine cell cycle sharing of 10,000 cells. Experiments were performed in three sets in duplicate wells and results are given in ± STD (n = 3).

2.1.2.5. Assessment of DNA fragmentation by TUNEL assay. Terminal deoxynucleotidyl transferase mediated dUTP nick end labeling (TUNEL) assay was used to determine the apoptosis with an aid of DNA fragmentation. For this, cells were incubated for 30 min at −20 °C to fix with ice cold ethanol (70%) and were washed with wash buffer. DNA labeling solution (50 μ) was added to cells and incubated for 60 min at 37 °C. Then the cells were rinsed with buffer and centrifuged for collection. Collected cells were resuspended in PI/RNase buffer (0.5 ml) at incubated at RT for 30 min. DNA fragmentation was analyzed by flow cytometry.

2.1.2.6. Assessment of mitochondrial membrane potential ($\Delta\Psi_m$). JC-1 (*BD Biosciences*, Catalog No. 551302) mitochondrial membrane potential sensor was to assess mitochondrial depolarization. Treated 1×10^6 cells/well MCF-7 cells were washed with PBS, trypsinized and collected by centrifugation. Cells were set with ice cold

70% ethanol and incubated for 30 min at −20 °C. 0.5 ml JC-1 working solutions was freshly prepared and added to each pellet. The pellets were then incubated in CO_2 incubator for 30 min at −20 °C. After washing with 1 ml assay buffer and suspended in 0.5 ml assay buffer. BD FACSCallibur was employed for mitochondrial membrane potential ($\Delta\Psi$ m) analysis.

2.1.2.7. Caspase-3 expression. After treatments 1 × 10^6 cells/well MCF-7 cells were incubated in dark with BD Biosciences, Caspase 3 – FITC for 60 min at room temperature. Cells were washed and suspended in PBS solution for Caspase3 expression analysis by BD FACSCallibur.

3. Results and discussion

3.1. Chemistry

The novel polycyclic cage-like hybrid heterocycle **4** has been derived through a synthetic strategy which involves dipole generation, [3 + 2] cycloaddition and a consequent annulation steps. The dipole, the non-stabilized azomethine ylide derived in situ from acenaphthenequinone **2** and 1,2,3,4-tetrahydroisoquinoline-3-carboxylic acid **3** reacts with *N*-unsubstituted 3,5-bis[(*E*)-phenylmethylidene]tetrahydro-4(1*H*)-pyridinone **1** through a [3 + 2] cycloaddition reaction affording the spirocycloadduct which upon subsequent annulation affords the novel polycyclic cage-like hybrid heterocycle **4** (Scheme 1). The reaction conditions optimized with [bmim]Br for the synthesis of analogues cage-like structures (Almansour et al., 2019) has been adopted here. Thus in an illustrative reaction, an equimolar mixture of **1**, **2** and **3** in 200 mg of [bmim]Br was subjected to microwave irradiation at 100 °C. The reaction advancement was observed after every 3 min intervals by TLC. After the reaction has been completed (12 min), the reaction mixture was extracted with ethyl acetate. As expected the reaction afforded the cage-like structure **4** in good yield (88%). The ionic liquid has been reused up to four times with only a very little loos in its catalytic activity. The structure of compound **4** was elucidated using spectroscopic studies. The probable mechanism for the formation of polycyclic cage-like heterocyclic hybrid **4** follows the same pathway as reported by us earlier (Almansour et al., 2019).

3.2. Biology

3.2.1. In vitro anticancer screening

Inhibition of cancer cells proliferation by compound **4** is assessed by MTT assay. The fact that, viable cells reduce MTT to purple formazan facilitates discrimination between viable and dead cells, ensuring the cytotoxicity of test drug. NCI-H460 (human non-small cancer), MCF-7 (Human breast cancer), HCT116 (Human colon cancer), Jurkat (Human T-cell lymphoma) cells were treated with different concentrations (1, 5, 10, 15 and 20 μM) of test compounds and the % cell viability is represented in Fig. 1. Cells without drugs and treated with 14 μM CPT (Camptothecin) were considered as negative and positive controls respectively.

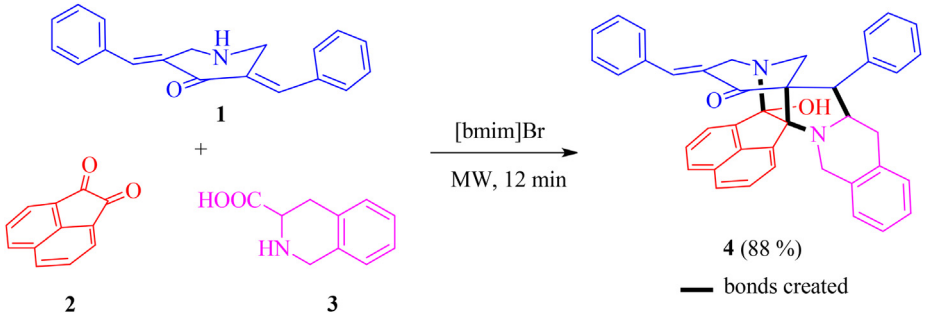

Scheme 1. Synthesis of polycyclic cage-like heterocyclic hybrid 4.

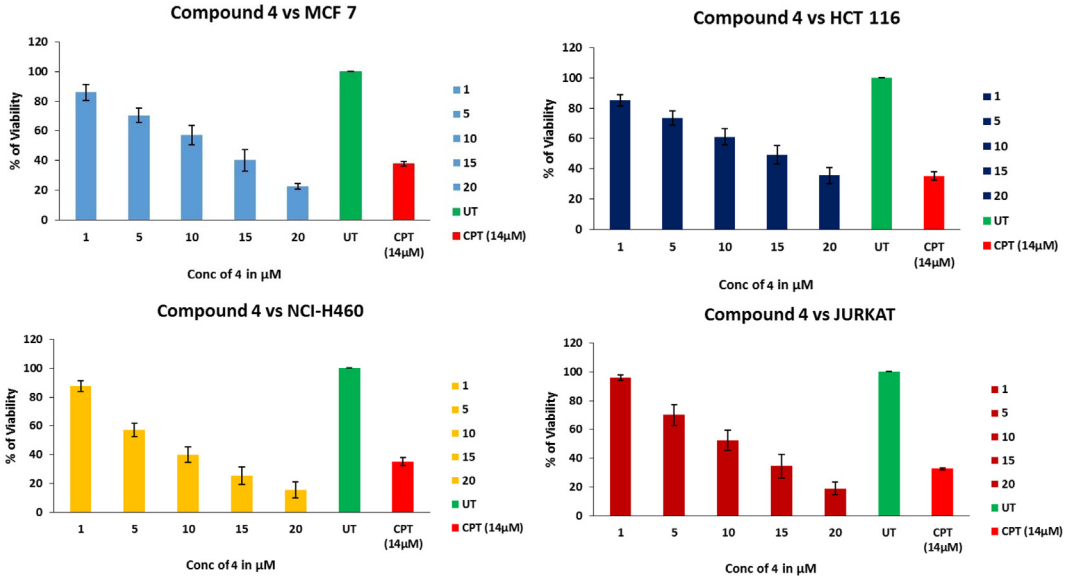

Fig. 1. % viability of cells as a function of test drug concentration, untreated cells and CPT as positive control via MTT assay.

As mentioned in Fig. 1 the % of cells viability decreased with increase in drug concentrations, where number of cages like structures will increase with increase in dose and trap the cancer cells into them. The mean the half maximal inhibitory concentration (IC_{50}) of compound **4** against 4 different cancer cell lines is represented in the Table 1. Among four cancer types, NCI-H460 has shown more sensitivity towards compound **4** after 48 h of incubation and the IC_{50} was found to be 8.9 ± 0.84 μm. Since compound **4** showed potential cytotoxicity towards NCI-H460 cell line, further studies related to cell death mechanism were performed on NCI-H460 cells.

Table 1
IC_{50} values of compound **4** against 4 different cell lines after 48 h of incubation.

Cell line	IC_{50} ± SD
HCT 116	13.3 ± 4.80
JURKAT	11.4 ± 1.90
MCF-7	11.7 ± 2.10
NCI-H460	8.9 ± 0.84

3.2.2. Apoptosis stimulation and DNA fragmentation analysis

Phosphatidyserine (PS) is disseminated in lipid bilayer cytosolic side of the cell membrane. PS tosses to cell's extracellular surface for early apoptotic and necrotic cells. This PS could be labeled using a most responsive early stage necrosis indicator, Annexin V-FITC. A nucleic acid dye, propidium iodide (PI) could not cross undamaged cell membranes. In other words, live cells and early stage apoptosis cells prohibit PI, whereas, late stage apoptotic and necrotic cells could be stained. Hence, use of double staining through Annexin

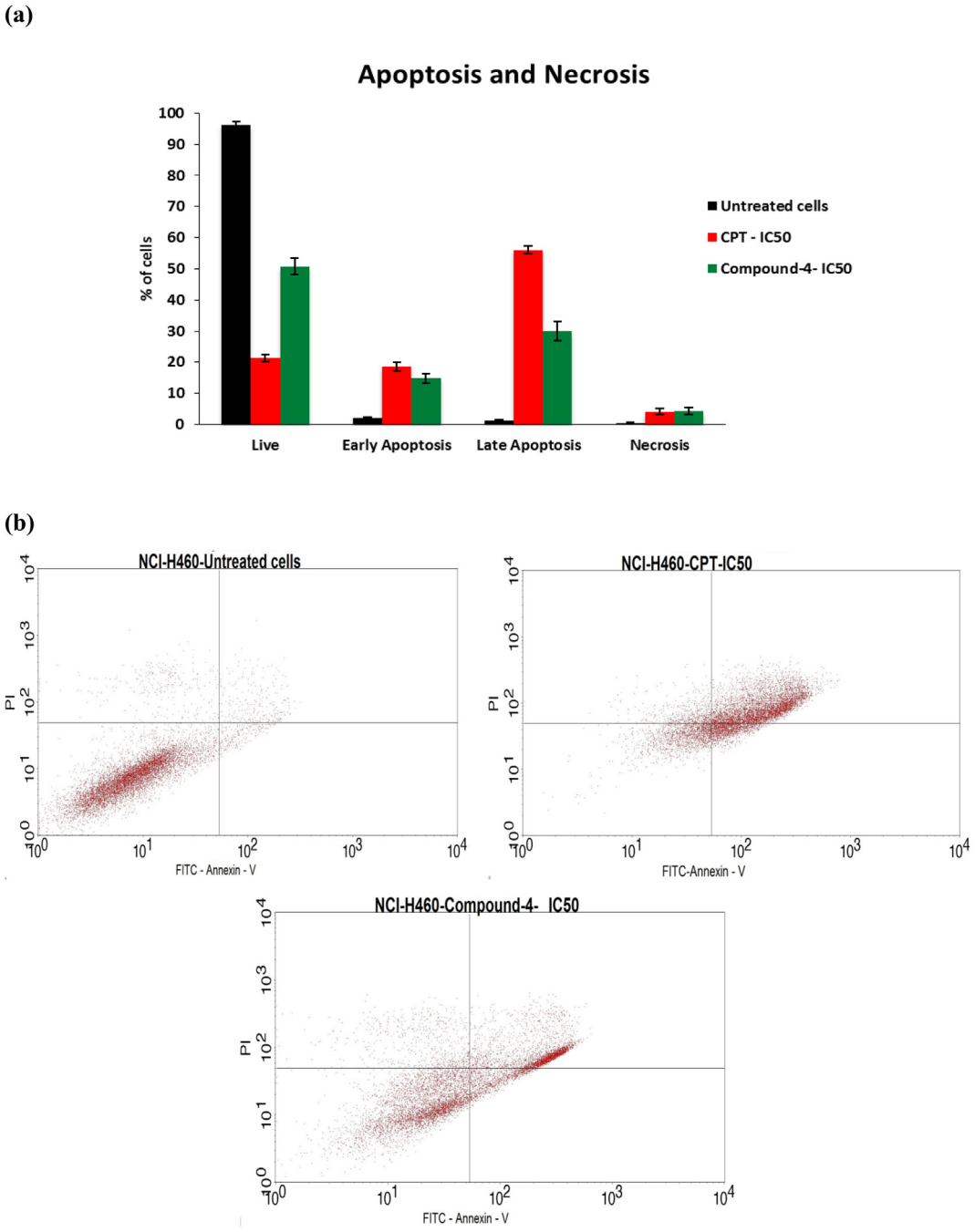

Fig. 2. a) % cells with respect to different stages of apoptosis, b) dot plot for the same.

V-FITC and PI, all stages of cells from live cells to necrotic cells will be differentiated by means of flow cytometry. Fig. 2a gives % of live, early stage and late apoptosis and necrosis cells for untreated, compound **4** treated and CPT treated cells. In Fig. 2b, flow cytometric analysis shows, live cells at lower left quadrant negative for both annexin V and PI, lower right quadrant gave early apoptosis, upper right gave late apoptotic cells. And upper left quadrant represents number of necrotic cells. As expected, % of live cells was more for untreated ones and was negligible for early and late apoptosis and for necrotic cells. CPT standard treatment showed less number of live cells compared to prepared test drug, almost same % of cells for early apoptosis and necrosis cells. However, for late apoptosis, CPT treated one showed 56.04% of cells and test drug treated one showed 30.04% of cells.

3.2.3. Assessment of mitochondrial membrane potential ($\Delta\Psi_m$) (MMP)

MMP is a key parameter to decide the mitochondrial function acting as a gauge to determine cell health. JC-1 is a cationic dye, lipophilic in nature. It has an ability to directly pierce into mitochondria and change the color from green to red with increased membrane potential. Healthy cells having high $\Delta\Psi_m$ allow JC-1 to form J-aggregate complexes giving red fluorescence. Whereas, unhealthy cells having low $\Delta\Psi_m$ does not form any complex and give green fluorescence due to depolarization of MMP. % depolarized cells as a function of untreated CPT treated and test drug treated conditions are given in Fig. 3. In a given dot plot, lower right quadrant gives population of depolarized cells and upper right one shows population of polarized cells.

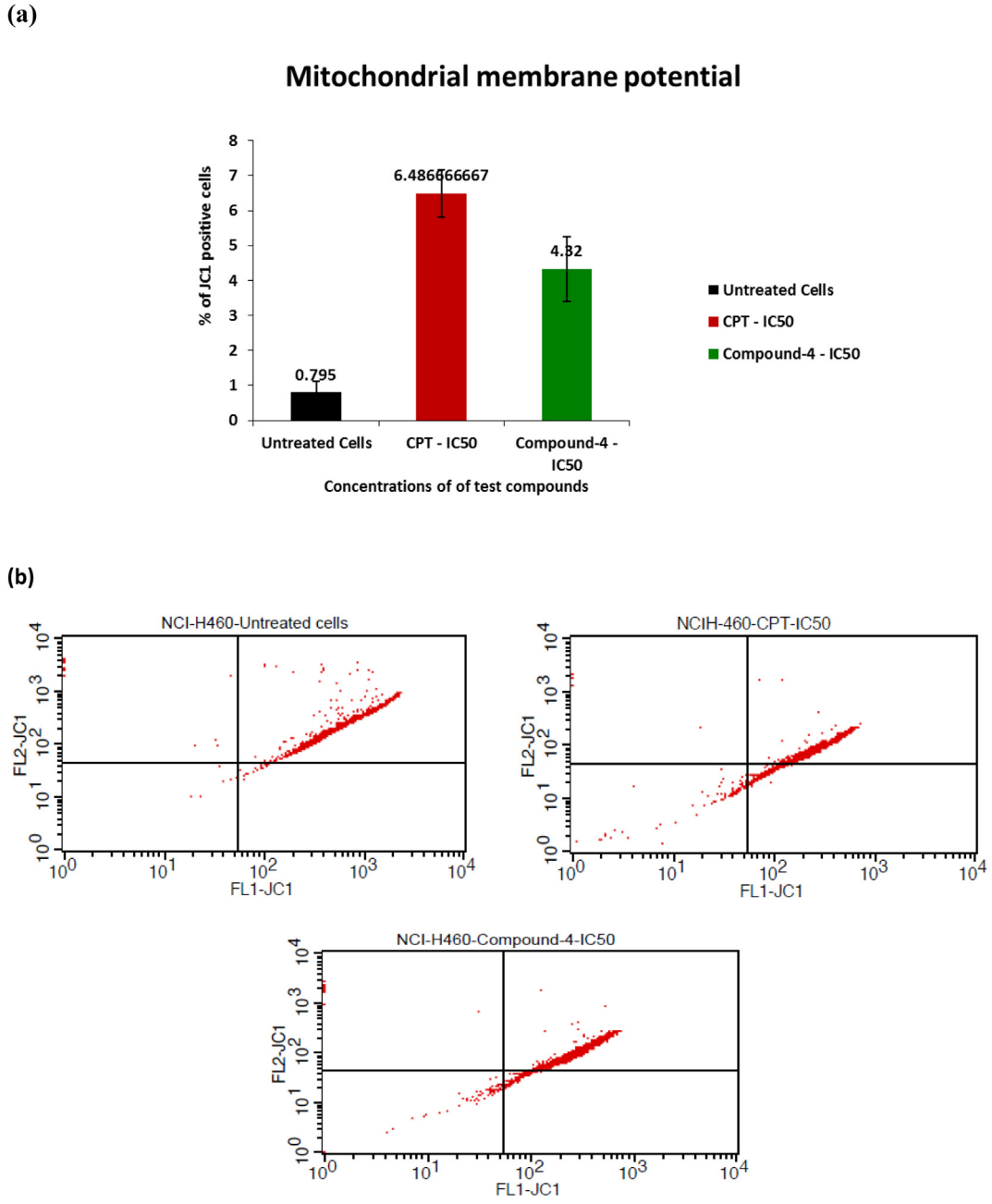

Fig. 3. a) % of JC-1 positive cells with respect to untreated, CPT treated and compound **4** treated cells, b) dot plot for the same.

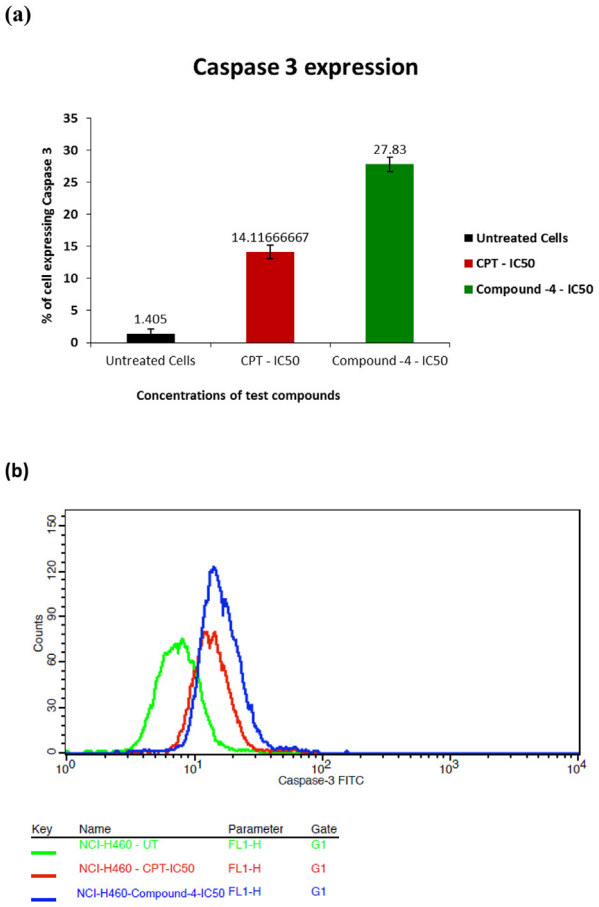

Fig. 4. a) % cells expressing caspase-3 with respect to IC_{50} concentrations of test compounds b) profile of % cells expressing the same.

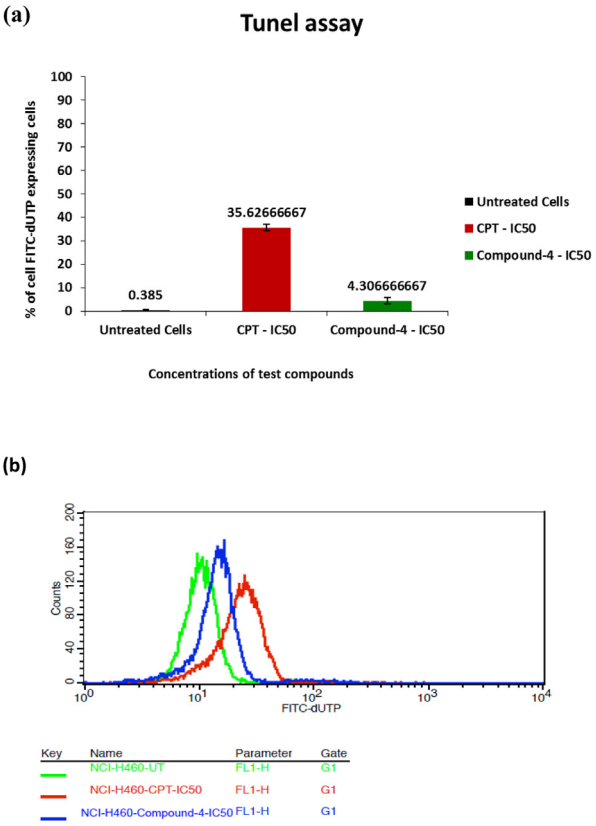

Fig. 5. a) % cells expressing FTIC-dUTP as a function of treatment conditions b) profile graph for the same.

3.2.4. Caspase-3 expression

For cell apoptosis, activation of caspase family is the key trend (Ferreira et al., 2000). Activated sub units proceed with deprivation of proteins and chromatin resulting in cell apoptosis in due course caspase-3 is a vital protease in human cell apoptosis as the prime effector and a reason for apoptosis (Takahashi, 1999; Porter and Jänicke, 1999). Caspase-3 expression for considered drug of IC_{50} is given in Fig. 4. Comparative to CPT, synthesized compound **4**-IC_{50} drug gave better caspase-3 expression (27.83%) than CPT (14. 11%) proving that mitochondrial lane is one of the major paths of cell apoptosis.

3.2.5. DNA fragmentation analysis by TUNEL assay

Fig. 5 gives percent cells expressing FITC-dUTP for untreated, test drug treated as well as CPT treated cells. Event though, compound **4** treated TUNEL staining showed better apoptosis (4.3%) than untreated cells (0.38%), the fragmentation was not remarkable comparative to CPT treatment which was 35.62%. Hence, it can be concluded that availability of free 3′ ends of fragmented DNA for the addition of dUTP nucleotides is less.

3.2.6. Cell cycle analysis

NCI-H460 cell cycle was observed to check the effect of compound **4** treatment and compared with CPT treatment. Main objective of this observation is to check whether compound **4** can direct NCI-H460 cell cycle to checkpoint phase. Cell cycle checkpoint control system rectifies anomaly in each step of cell cycle, that can assist to avert the cells enters to the later step in the DNA damage. Failure of cell cycle checkpoint control system occurs in each stage of cancer cell cycle so that DNA replication will be discarded and mitosis will be inhibited in spite of DNA impairment. This leads to uncontrollable proliferation of cancer cells (Worthley et al., 2007). Fig. 6 gives flow cytometry results analyzed for different phases of cells using PI as a fluorescence probe. The increased accumulation of cells at IC_{50} dosage of synthesized test drug shows the inhibition of cell cycle at G2/M phase which was 28.89%. AT synthesis phase it was 27.84%, where as in G0/G1 phase, accumulation 18.83% which was very much lesser than untreated and CPT treated cells. The depletion of cells was found in sub G0/G1 phase compared to CPT treated cells. Cell cycle results showed that, DNA were damaged and hence DNA replication was not appropriate.

4. Conclusions

A novel polycyclic cage-like hybrid heterocycle has been synthesized through a synthetic strategy which involves dipole generation, [3 + 2] cycloaddition and a subsequent annulation steps. The structural confirmation was done by spectroscopic techniques. The polycyclic cage-like hybrid heterocyclic compound was then evaluated for *in vitro* anticancer activity. Cell viability was concentration dependent, as analyzed by MTT assay. Annexin V and PI double staining gave stages of apoptosis, where, test drug showed nearby effect as CPT at early apoptosis, but one fold lower for late apoptosis. Number of cells showing caspase-3 expression was higher for compound **4** treated ones indicating the mitochondrial

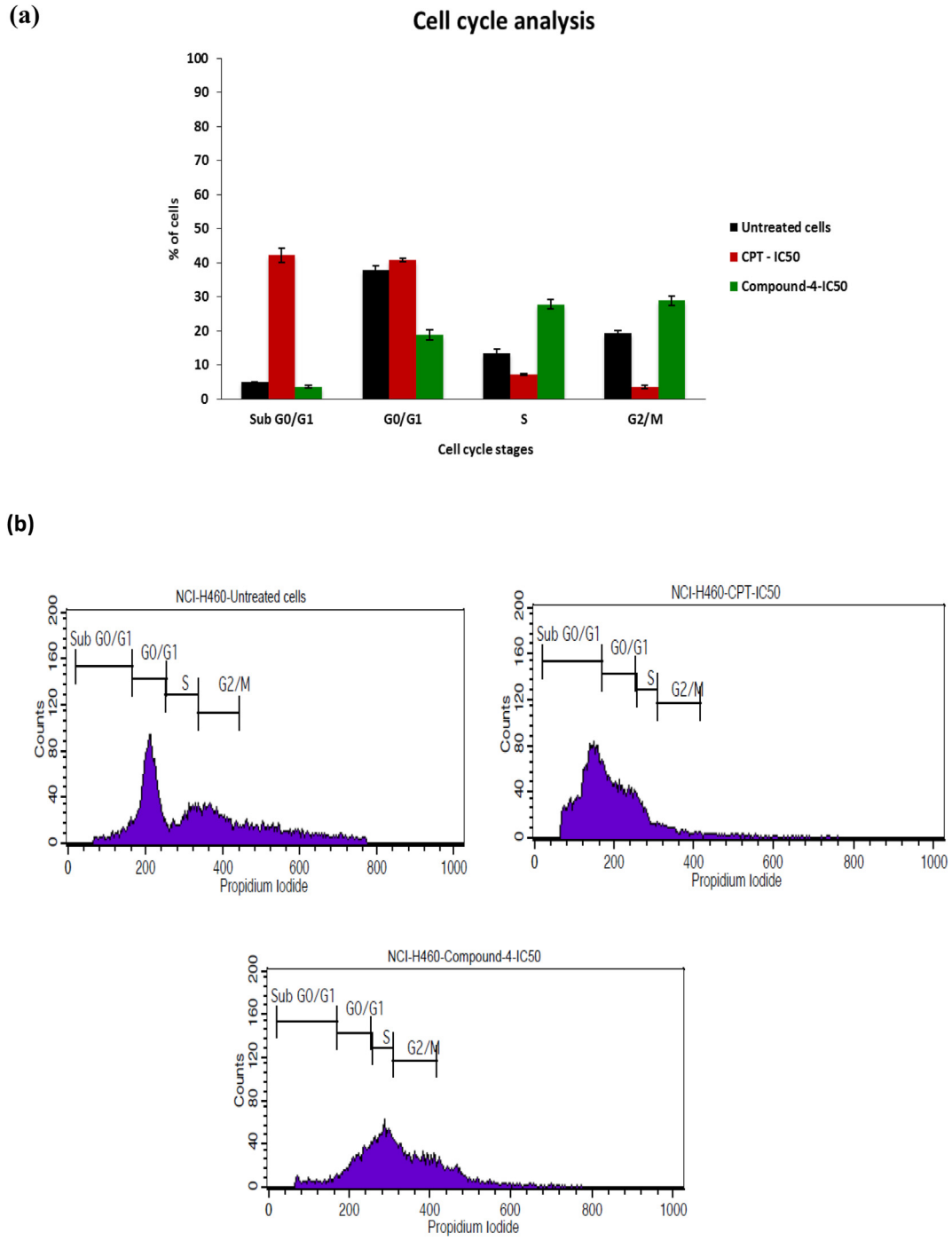

Fig. 6. a) Cancer cells cycle changes distribution and Induction of cell death among untreated, CPT treated and compound **4** treated cells, b) distribution profile of different cell cycle stages.

attack path way as the major route of apoptosis. In conclusion, the synthesized polycyclic cage-like hybrid heterocycle showed a better anticancerous activity via, DNA damage as well as mitochondrial deprivation. The anticancer activity of derivatives of this cage-like compound with different cell lines is under progress and will be published in due course.

Declaration of Competing Interest

The authors declare that they have no known competing financial interests or personal relationships that could have appeared to influence the work reported in this paper.

Acknowledgment

The project was supported by Researchers Supporting Project number (RSP-2019/142), King Saud University, Riyadh, Saudi Arabia. The authors also thank Stellixir Biotech Pvt. Ltd, Bangalore, India for performing the biological assays.

References

Alfuraydi, A.A., Devanesan, S., Al-Ansari, M., AlSalhi, M.S., Ranjitsingh, A.J., 2019. Eco-friendly green synthesis of silver nanoparticles from the sesame oil cake and its potential anticancer and antimicrobial activities. J. Photochem. Photobiol. B. 192, 83–89.

Ali, I., Lone, M.N., Alothman, Z.A., Alwarthan, A., 2017. Insights into the pharmacology of new heterocycles embedded with oxopyrrolidine rings: DNA binding, molecular docking, and anticancer studies. J. Mol. Liq. 234, 391–402.
Ali, I., Nadeem Lone, M., Suhail, M., Danish Mukhtar, S., Asnin, L., 2016. Advances in nanocarriers for anticancer drugs delivery. Curr. Med. Chem. 23, 2159–2187.
Almansour, A.I., Kumar, R.S., Arumugam, N., Kotresha, D., Menendez, J.C., Anti-Cancer compound, US Patent US 10,357,485 B1 Jul. 23, 2019.
Androutsopoulos, V.P., Spandidos, D.A., 2018. Anticancer pyridines induce G2/M arrest and apoptosis via p53 and JNK upregulation in liver and breast cancer cells. Oncol. Rep. 39, 519–524.
AlSalhi, M.S., Devanesan, S., Alfuraydi, A.A., Vishnubalaji, R., Munusamy, M.A., Murugan, K., Nicoletti, M., Benelli, G., 2016. Green synthesis of silver nanoparticles using Pimpinella anisum seeds: antimicrobial activity and cytotoxicity on human neonatal skin stromal cells and colon cancer cells. Int. J. Nanomedicine. 11, 4439–4449.
Boros, E., Rybak-Akimova, E., Holland, J.P., Rietz, T., Rotile, N., Blasi, F., Day, H., Latifi, R., Caravan, P., 2013. Pycup A bifunctional, cage-like ligand for 64Cu radiolabeling. Mol. Pharm. 11, 617–629.
Boschelli, D.H., Wang, D.Y., Ye, F., Yamashita, A., Zhang, N., Powell, D., Weber, J., Boschelli, F., 2002. Inhibition of Src kinase activity by 4-anilino-7-thienyl-3-quinolinecarbonitriles. Bioorg. Med. Chem. Lett. 12, 2011–2014.
Ferreira, C.G., Span, S.W., Peters, G.J., Kruyt, F.A., Giaccone, G., 2000. Chemotherapy triggers apoptosis in a caspase-8-dependent and mitochondria-controlled manner in the non-small cell lung cancer cell line NCI-H460. Cancer Res. 60, 7133–7141.
Fukusumi, H., Handa, Y., Shofuda, T., Kanemura, Y., 2019. Evaluation of the susceptibility of neurons and neural stem/progenitor cells derived from human induced pluripotent stem cells to anticancer drugs. J Pharmacol Sci. 140, 331–336.
Geldenhuys, W.J., Malan, S.F., Bloomquist, J.R., Marchand, A.P., Van der Schyf, C.J., 2005. Pharmacology and structure-activity relationships of bioactive polycyclic cage compounds: a focus on pentacycloundecane derivatives. Med. Res. Rev. 25, 21–48.
Hamilton, G., Rath, B., 2014. A short update on cancer chemoresistance. Wiener Medizinische Wochenschrift 164, 456–460.
Han, Q.-B., Xu, H.-X., 2009. Caged Garcinia xanthones: development since 1937. Curr. Med. Chem. 16, 3775–3796.
Li, L.-N., Wang, L., Cheng, Y.-N., Cao, Z.-Q., Zhang, X.-K., Guo, X.-L., 2018. Discovery and characterization of 4-hydroxy-2-pyridone derivative sambutoxin as a potent and promising anticancer drug candidate: activity and molecular mechanism. Mol. Pharm. 15, 4898–4911.
Lv, Z., Zhang, Y., Zhang, M., Chen, H., Sun, Z., Geng, D., Niu, C., Li, K., 2013. Design and synthesis of novel 2′-hydroxy group substituted 2-pyridone derivatives as anticancer agents. Eur. J. Med. Chem. 67, 447–453.
Nien, C.-Y., Chen, Y.-C., Kuo, C.-C., Hsieh, H.-P., Chang, C.-Y., Wu, J.-S., Wu, S.-Y., Liou, J.-P., Chang, J.-Y., 2010. 5-Amino-2-aroylquinolines as highly potent tubulin polymerization inhibitors. J. Med. Chem. 53, 2309–2313.
Petrelli, A., Valabrega, G., 2009. Multitarget drugs: the present and the future of cancer therapy. Expert Opin. Pharmacother. 10, 589–600.
Porter, A.G., Jänicke, R.U., 1999. Emerging roles of caspase-3 in apoptosis. Cell Death Differ. 6, 99–104.
Priyadarshani, G., Nayak, A., Amrutkar, S.M., Das, S., Guchhait, S.K., Kundu, C.N., Banerjee, U.C., 2016. Scaffold-hopping of aurones: 2-arylideneimidazo [1, 2-a] pyridinones as topoisomerase IIα-inhibiting anticancer agents. ACS Med. Chem. Lett. 7, 1056–1061.
Pulkkinen, M., Pikkarainen, J., Wirth, T., Tarvainen, T., Haapa-aho, V., Korhonen, H., Seppälä, J., Järvinen, K., 2008. Three-step tumor targeting of paclitaxel using biotinylated PLA-PEG nanoparticles and avidin–biotin technology: formulation development and in vitro anticancer activity. Eur. J. Pharm. Biopharm. 70, 66–74.
Rostom, S.A., Faidallah, H.M., Al-Saadi, M.S., 2011. A facile synthesis of some 3-cyano-1, 4, 6-trisubstituted-2 (1H)-pyridinones and their biological evaluation as anticancer agents. Med. Chem. Res. 20, 1260–1272.
Saleem, K., Wani, W.A., Haque, A., Milhotra, A., Ali, I., 2013. Nanodrugs: magic bullets in cancer chemotherapy. Topics Anti Cancer Res. 58, 437–494.
Solomon, V.R., Lee, H., 2009. Chloroquine and its analogs: a new promise of an old drug for effective and safe cancer therapies. Eur. J. Pharmacol. 625, 220–233.
Solomon, V.R., Lee, H., 2011. Quinoline as a privileged scaffold in cancer drug discovery. Curr. Med. Chem. 18, 1488–1508.
Takahashi, A., 1999. Caspase: executioner and undertaker of apoptosis. Int. J. Hematol. 70, 226–232.
Varmus, H., 2006. The new era in cancer research. Science 312, 1162–1165.
Wissner, A., Mansour, T.S., 2008. The development of HKI-272 and related compounds for the treatment of cancer. Archiv der Pharmazie: Int. J. Pharm. Med. Chem. 341, 465–477.
Worthley, D.-L., Whitehall, V.-L., Spring, K.-J., Leggett, B.-A., 2007. Colorectal carcinogenesis: road maps to cancer. World J. Gastroenterol. 13, 3784–3791.
Yihebali, C., Zhan, X.-K., Hao, Y., Xie, G.-R., Wang, Z.-Z., Wei, X., Wang, Y.-G., Xiong, F.-X., Hu, J.-F., Lin, Y., 2013. An open-labeled, randomized, multicenter phase IIa study of gambogic acid injection for advanced malignant tumors. Chin. Med. J. 126, 1642–1646.